

Tribological characteristics of few layers graphene over Ni grain and interface boundaries

Electronic Supplementary Information (ESI)

M. Tripathi¹, F. Awaja¹, G. Paolicelli², R. Bartali¹, E. Iacob¹, S. Valeri³, S. Ryu⁴, S. Signetti⁵,
G. Speranza¹, N.M. Pugno^{5,1,6,*}

¹ Centre for Materials and Microsystems, Fondazione Bruno Kessler, via Sommarive 18, I-38123 Povo (Trento), Italy

² Istituto Nanoscienze, Consiglio Nazionale delle Ricerche, via Campi 213/A, I-41125 Modena, Italy

³ Department of Physical, Informatics and Mathematical Sciences, Università di Modena e Reggio Emilia, Via Campi 213/A, I-41125 Modena, Italy

⁴ Korea Advanced Institute of Science and Technology, Daejeon 305-338, Korea

⁵ Laboratory of Bio-Inspired and Graphene Nanomechanics, Department of Civil, Environmental and Mechanical Engineering, University of Trento, via Mesiano 77, I-38123 Trento, Italy,

⁶ School of Engineering and Materials Science, Queen Mary University of London, Mile End Road, E1 4NS London, UK

*Corresponding author: nicola.pugno@unitn.it

Morphological description of bare polycrystalline Ni and CVD grown graphene on polycrystalline Ni

The existence of flat areas and rough or stepped regions on CVD grown graphene is highlighted applying a local derivative operator (Gwyddion 2.38 open software, <http://gwyddion.net/>) to the raw topography data (Figure S1a). In the Figure S1, we present this procedure applied to Figure 1c of the manuscript. The procedure has been started from topography image (figure S1a). Then the results of the local derivative operator are shown in Figure S1b. Colour scale represents the local surface slope so that flat regions appear uniform and darker respect to steps and edges. From this analysis, it is evident that flat and uniform graphene regions (that we will refer to as graphene grain in the manuscript) are surrounded and separated by extended rough regions (graphene interface boundary IB in the manuscript). Graphene grains are characterised by a uniform and small slope

(brown regions) and because of their shape and size seems matching a single Ni grain. A statistical analysis reveals that graphene grain possess a typical lateral dimension between 500 and 1000 nm. The superposition over the local slope image (panel b) of the friction mask representing areas characterized by high friction values clearly shows that graphene grain possesses higher friction respect to graphene interfacial grain boundaries (IB).

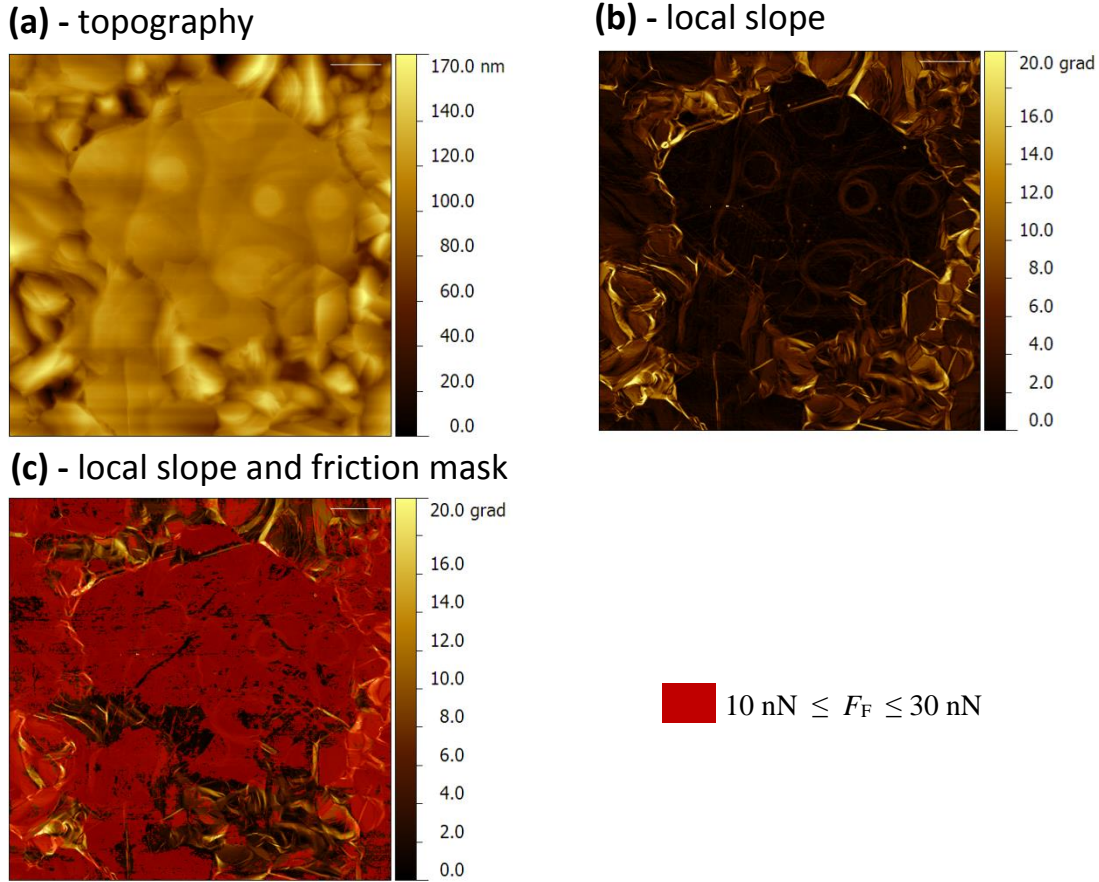


Figure S1: Procedure for the determination of substrate topography and related friction force signals. (a) Topography AFM image of a 15x15 μm² graphene region measured in contact mode. (b) Local derivative operator applied directly to the raw topography data. Color scale represents the local surface slope so that flat regions appear uniform and darker with respect to steps and edges. (c) Superposition over the local slope image (panel b) of a friction mask where red regions represent areas characterized by friction values between 10 and 30 nN.

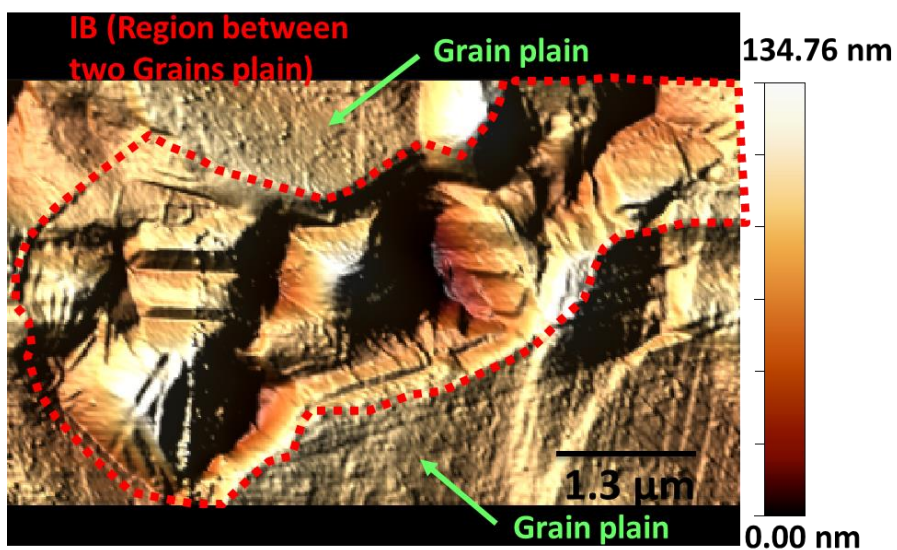


Figure S2: Intermittent contact mode, high resolution (steps/line 1024), 3D topographic image (6.5 x 3.8 μm²) of Gr/Ni-P sample. Green colour arrows are showing region of graphene covered grain plains of polycrystalline Ni. Within grains a region we refer to as Ni interface boundary (IB) is highlighted by the red colour dashed line. This region is separated by Ni grain and is highly disordered relatively to the flat surface of the grain plain. It comprises of a lump of carbon layers equivalent or higher than grain altitude (brightest colour as confirmed by scale bar). The width of IB region varies from 1 μm to 2.5 μm that include irregular carbon steps, plateaus and other irregular structures.

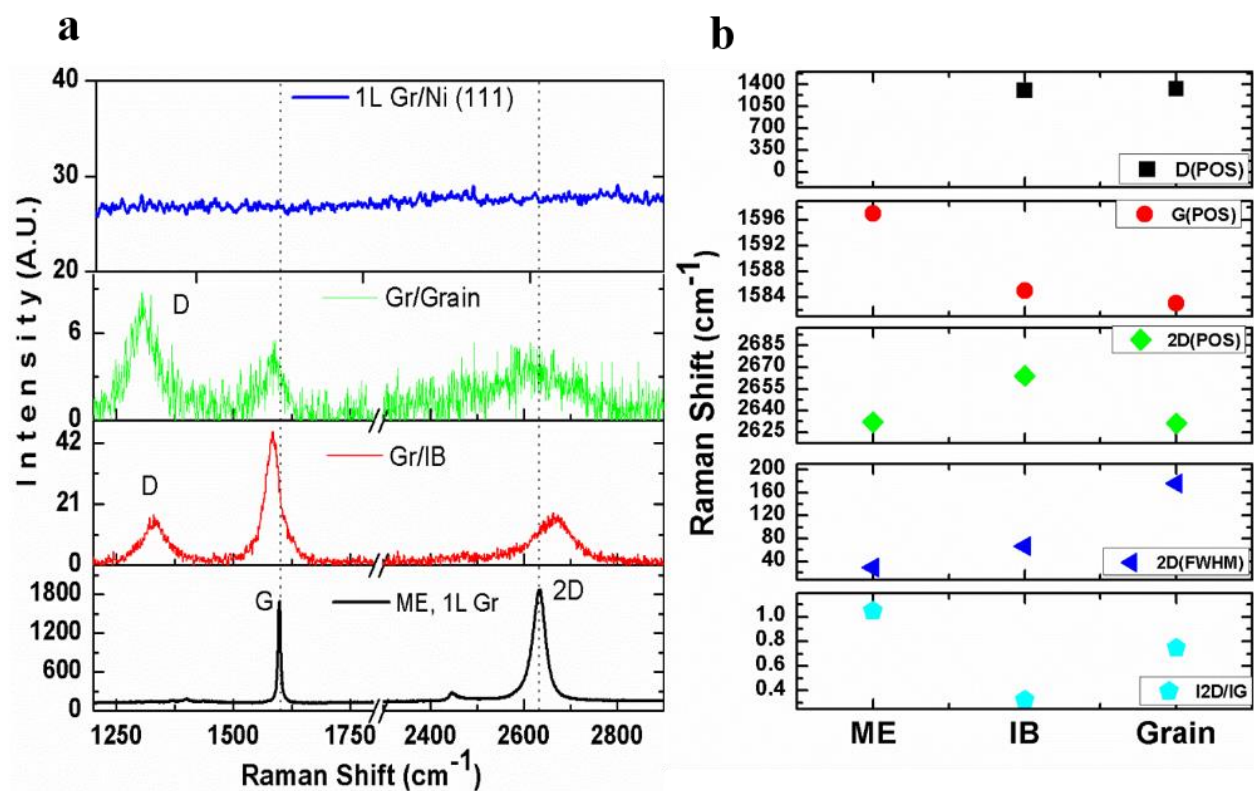


Figure S3: Raman spectra for evaluation of thickness of graphene layers over Gr/Ni-P along with reference, 1L Gr/SiO₂ and 1L Ni (111). (a) Raman Spectra of 1L graphene on Ni crystal, FLG on region of grain and interfacial boundaries (IB) and mechanically exfoliated 1L graphene on Silica. Graphene on silica shows relatively sharp peaks of G (~ 1597 cm⁻¹) and 2D (~ 2633 cm⁻¹) with no disorder induced peak (D). Spectra from 1L graphene over Ni crystal show suppression of all defined peaks. FLG shows presence of D, G and 2D peaks at ~ 1333 cm⁻¹, ~ 1587 cm⁻¹ and ~ 2667 cm⁻¹ respectively. The 2D peak is relatively suppressed at grain region with respect to interfacial boundaries. Vertical dashed line reveals shifting of peak positions (G and 2D) in CVD produced graphene with respect to mechanically exfoliated (ME) 1L graphene. (b) Quantitative values of peak position (POS) of D, G and 2D respectively from panel (a) with ratio of intensities between 2D and G peak (I_{2D}/I_G) and FWHM (full width of half maximum) using Lorentzian fitting.

Figure S3 shows μ -Raman spectra carried out at 1L graphene on Ni crystal (Ni (111)), silica substrate and FLG on grain and IB over polycrystalline Ni. Raman spectra for mechanically exfoliated 1L graphene on silica and CVD produced 1L graphene on Ni crystal are two extreme examples of graphene strain that influence the phononic vibration of carbon atoms. We observed total suppression of Raman shift peaks for 1L graphene on Ni crystal. For 1L graphene on silica, Raman shift peaks like G ($\sim 1597 \text{ cm}^{-1}$) and 2D ($\sim 2633 \text{ cm}^{-1}$) are clearly visible with no disorder induced peak (D). Raman spectrum for Gr/Ni-P lies in these two extreme cases, since it is influenced from Ni substrate, therefore, base line correction has been performed to eliminate background influence. The Raman shift of D, G and 2D peaks are observed at $\sim 1333 \text{ cm}^{-1}$, $\sim 1587 \text{ cm}^{-1}$ and $\sim 2667 \text{ cm}^{-1}$ respectively. These wave numbers are relatively deviated from the spectra obtained from ME graphene used as a reference (Figure S3(b)). Multilayer graphene flakes formed on polycrystalline Ni films are usually stacked with deviations from the Bernal stacking type and show misorientation among the carbon layers¹. Further, the doping (p-type) due to Ni metal for producing strain cannot be neglected². The suppression of 2D peaks at the grain regions relative to IB has been observed. The peak of vibrational G band is attributed to the bond stretching of all pairs of sp² atoms in both rings and chains form. However, suppression of 2D peak is associated with stronger chemical interaction, i.e. hybridization of the metal d-band with graphene π -states². For one layer graphene on Ni (111), the chemical interaction between graphene and Ni leads to a large energy difference in the p_z orbital of graphene and a loss of the resonance conditions for Raman². Consequently, no Raman signal for graphene on Ni (111) is observed under similar instrumental set-up ($\lambda = 632.8 \text{ nm}$). In such situation, it is complex to calculate quantitative values of graphene thickness over Ni substrate. Nevertheless, qualitative estimation of graphene thickness and the presence of sp² bonded carbon layers is feasible using intensity ratio I_{2D}/I_G. From Figure S3(b), the intensity ratio of 2D/G confirms that IB has higher accumulation of carbon layers than grain region; therefore the lateral force F_L contrasts (as describe in main text) obtained above arise from difference in thickness distribution of carbon layers and not from heterogeneity of the system.

In order to validate our argument for the suppression of the Raman 2D peak on Ni substrate, we performed Raman map of CVD produced graphene on Ni and transferred over silica (Gr/Si-T) through wet chemical procedure³. The optical image is shown in Figure S4(a): Raman probed spots ($\sim 1 \mu\text{m}$ in diameter step) are labelled from A1 to E5. Its topographic image (rotated AFM image Figure S4(b)) reveals that brighter optical contrast has higher altitude (Z-direction) which can

originate from IB as discussed above. Raman map in such realm has scarce monolayer graphene (only at location “D4 with $I_{2D}/I_G \geq 1$ ”) available (Figures S4(c) and S4(d)). The IB has a range of 4-7 (higher altitude region) and grain of 2-4 carbon layers under laser probe size of $\sim 1 \mu\text{m}$. Throughout investigation of Raman map no such suppression of 2D peaks has been observed relative to G and D peaks unlike Gr/Ni-P.

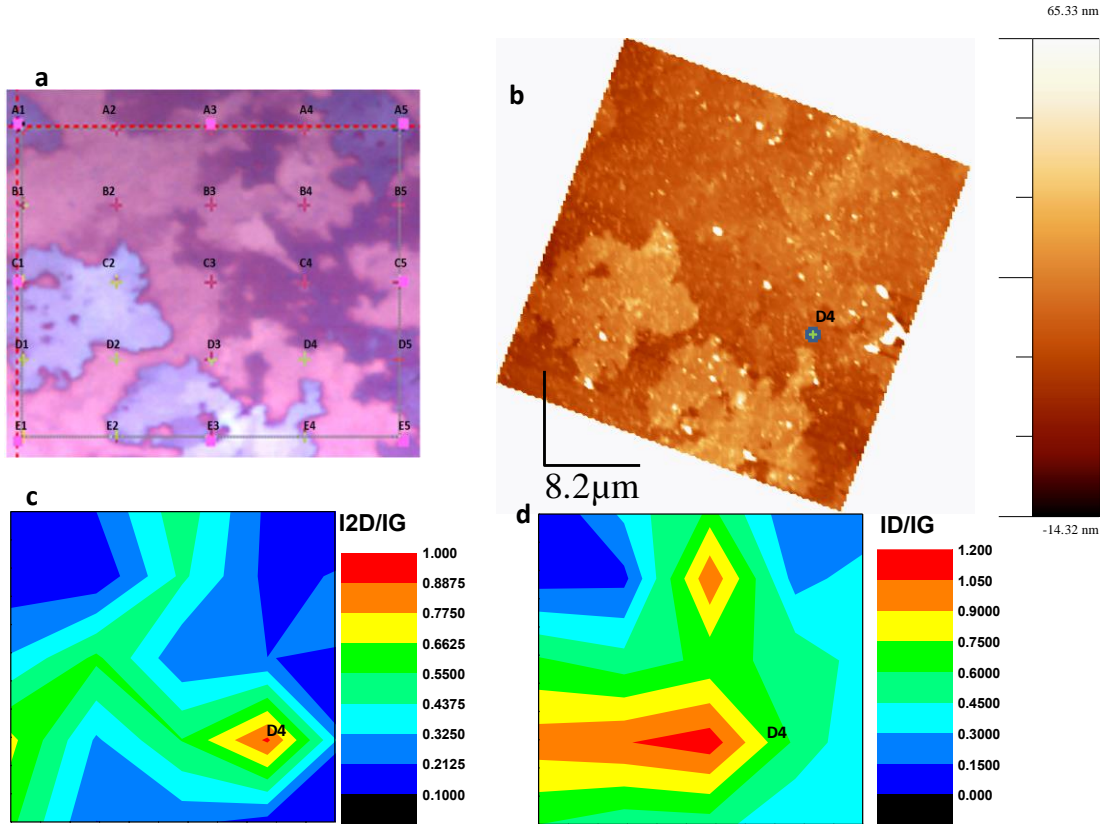


Figure S4: Raman mapping of CVD produced graphene on polycrystalline Ni and transferred to SiO_2 .

(a) Optical image of CVD produced FLG on Ni and transferred over silica substrate (Gr/Si-T). The red colour dashed rectangle corresponds to the area on which programmed Raman map has been carried out ($\approx 20 \times 20 \mu\text{m}^2$). The alphanumeric characters (A1 to E5) identify the Raman probe positions. (b) Tapping mode (flattened, height channel), the same region has been relocated in AFM apparatus. The topographic image has been aligned vertically for better comparison with optical image of panel (a). (c) Intensity ratio of Raman peak (2D/G) corresponding to position D4. (d) Intensity ratio of Raman peak (D/G). Position D4 shows 1L graphene (confirm from panel (c)) and its appearance in optical image (pink colour in panel (a)) and AFM topography in panel (b)). Note that the resolution of panel (c) and (d) is not equivalent to panel (b) since distance between each Raman probed spot is $4 \mu\text{m}$.

Finite element (FEM) simulations

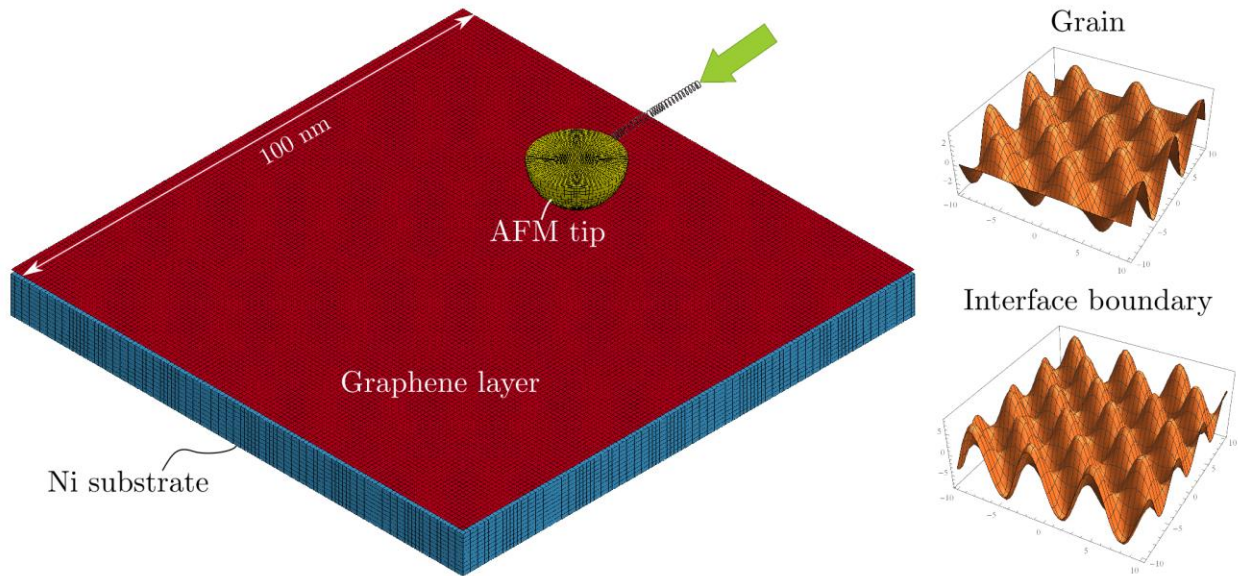


Figure S5: FEM simulations setup. The sliding tip is subjected to a constant imposed velocity which is applied on an auxiliary node linked to the hemisphere with a horizontal spring: this scheme allows to easily compute the friction force signal as the force acting in the spring during the sliding motion. The normal force is applied directly on the tip. The overall tip sliding displacement is of 50 nm, starting and terminating 25 nm far from the edges, which are fully clamped at the area edges. The substrate is also fixed at the base, blocking the vertical motion. The roughness of the substrate is translated in an equivalent sinusoidal surface in both the in-plane directions. The parameters defining the surface differ between grain and interfacial boundaries according to the experimental measured average roughness R_a (portions of the resulting profiles of 10x10 nm are depicted in the figure).

References

1. Zhang, Y.; Gao, T.; Xie, S.; Dai, B.; Fu, L.; Gao, Y.; Chen, Y.; Liu, M.; Liu, Z., Different growth behaviors of ambient pressure chemical vapor deposition graphene on Ni(111) and Ni films: A scanning tunneling microscopy study. *Nano Research* **2012**, *5* (6), 402-411.
2. Dahal, A.; Batzill, M., Graphene-nickel interfaces: a review. *Nanoscale* **2014**, *6* (5), 2548-62.
3. Li, X.; Zhu, Y.; Cai, W.; Borysiak, M.; Han, B.; Chen, D.; Piner, R. D.; Colombo, L.; Ruoff, R. S., Transfer of Large-Area Graphene Films for High-Performance Transparent Conductive Electrodes. *Nano Letters* **2009**, *9* (12), 4359-4363.